THE JOURNAL OF PHYSICAL CHEMISTRY C

Article

pubs.acs.org/JPCC

Structural and Band Gap Investigation of GaN:ZnO Heterojunction Solid Solution Photocatalyst Probed by Soft X-ray Spectroscopy

E. J. McDermott,*[,†] E. Z. Kurmaev,[‡] T. D. Boyko,[†] L. D. Finkelstein,[‡] R. J. Green,[†] K. Maeda,[¶,§] K. Domen,[¶] and A. Moewes[†]

[†]Department of Physics and Engineering Physics, University of Saskatchewan, 116 Science Place, Saskatoon, Saskatchewan S7N 5E2, Canada

[‡]Institute of Metal Physics, Russian Academy of Sciences-Ural Division, 620990 Yekaterinburg, Russia

[¶]Department of Chemical System Engineering, The University of Tokyo, 7-3-1 Hongo, Bunkyo-ku, Tokyo 113-8656, Japan

[§]Precursory Research for Embryonic Science and Technology (PRESTO), Japan Science and Technology Agency (JST), 4-1-8 Honcho Kawaguchi, Saitama 332-0012, Japan

ABSTRACT: We have studied the electronic structure of $(Ga_{1-x}Zn_x)$-$(N_{1-x}O_x)$ as a function of zinc and oxygen concentration (x) using soft X-ray emission (XES) and absorption (XAS) spectroscopy. We have constructed a binding energy model of the compound's valence band using common metal features found in both N K and O K XES spectra. By comparing the spectra with theoretical DFT models, we determine that our measurements describe an inverted gap heterostructure of GaN and ZnO with two optical gaps characteristic of each phase, 2.6 and 2.8 eV, respectively. We observe a band gap reduction of 0.4 eV across the range of x tested, which is attributed to repulsion between each phase's conduction band onset due to the proximity of states at the phase interface.

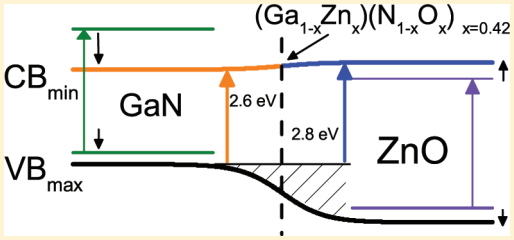

INTRODUCTION

Compounds of GaN and ZnO have recently attracted attention as promising photocatalyst candidates for solar-driven water splitting, with possible applications in alternative energy production.[1,2] To efficiently generate photocurrent from the solar spectrum (with a peak intensity at 2.5 eV) while simultaneously driving the water splitting reaction (requiring at least 1.23 eV of potential[3]), a photocatalyst with a band gap in the vicinity of 2.0 eV is desired. While photocatalyic activity is found in several metal oxide systems,[4] most have band gaps of greater than 3 eV, limiting photoabsorption to the UV portion of the spectrum. However, metal oxides can have other desirable properties as energy materials, such as photostability and an appropriate conduction band energy for H+ reduction to H_2.[5] Therefore, the search for metal oxide photocatalysts with reduced band gap is of great practical interest.

ZnO has an appropriate conduction band position for H_2 production[5] but is unsuitable as a visible-light photocatalyst because its optical band gap is too large ($E_{gap} \approx 3.3$ eV[6]). This band gap can be attributed to the positioning of Zn 3d deep within the valence band (8 eV below the Fermi level); this attracts O 2p valence states to lower orbital energy, away from the material's conduction band. However, N 2p states have a higher orbital energy than O 2p states, so it has been hypothesized that zinc oxynitrides would exhibit a reduced band gap compared to ZnO,[5] with nitrogen states dominating the top of the valence band.

While GaN is also a wide-gap semiconductor ($E_{gap} = 3.4$ eV), like ZnO it is also a d^{10} metal cation system with the same wurtzite structure.[7] This suggests that a solid solution of GaN and ZnO could approximate the desired zinc oxynitride material. It has been found that the combination produces a material with a band gap dependent on the compositional ratio of Ga to Zn.[8] For these GaN:ZnO compounds, E_{gap} values as low as 2.6−2.8 eV have been measured experimentally in GaN-rich samples by UV−vis diffuse reflectance.[5] This is a 0.5−0.8 eV band gap reduction over either precursor material, suggesting that an intermediate phase of GaN:ZnO may form. An E_{gap} as low as 2.37 eV has been observed in ZnO-rich compositions.[9] In addition, photoluminescence spectroscopy has revealed the presence of two luminescence bands at approximately these photon energies, which suggests either a material with a significant population of defect states, as Yoshida et al. surmised,[10] or a nonhomogeneous solid with more than one optical gap. While XEOL spectroscopy supports the proposal that Zn and O acceptor and donor sites contribute to the PL spectrum, it is not clear that this channel contributes to the photoabsorption of the material, as the XEOL peak is centered at 2.0 eV, below the UV−vis band gap value.[11]

The origins of band gap reduction in GaN:ZnO compounds have yet to be fully explained in the literature. Density functional theory (DFT) calculations of the electronic structure of proposed GaN:ZnO oxynitride defect superlattices were shown to underestimate the UV−vis band gap,[10,12] but this is

Received: February 7, 2012
Revised: March 14, 2012
Published: March 16, 2012

typical for DFT calculations in wide-gap semiconductors.[13] It has been previously shown that the large band gap of transition metal semiconductors,[14] in particular, ZnO[15] and GaN,[16] originates from interactions between anion 2p states and cation 4s states in the valence band. On the other hand, it was previously believed that in ZnO-doped GaN the Zn 3d states would strongly couple with the N 2p states, pushing up the valence-band maximum in energy, resulting in band gap reduction. These strong 2p−3d couplings present a challenge for DFT calculations, complicating electronic property calculations of these materials from first principles.[17] An alternative theory of band gap reduction in this system is that the visible-light absorption of GaN-rich GaN:ZnO occurs via electron transitions from a Zn acceptor level to the conduction band; this theory is also based on DFT calculations as well as low-temperature UV−visible diffuse reflectance.[10,18,19] More recent work consists of DFT simulations that examine ZnO and GaN phase formations by Monte Carlo methods[20] and the effects of potential phase interfaces,[21] strengthening the theoretical evidence for a disordered system rather than an oxynitride superlattice.

Due to the relevance of GaN:ZnO as a viable photocatalyst and the conflicting explanations of its electronic structure in the literature, it is important to study this electronic structure as directly as possible. In this work, we report the first experimental study of the electronic structure of a GaN:ZnO compound combining both soft X-ray emission (XES) and absorption (XAS) spectroscopy in an attempt to clarify the origin of its band gap reduction. The hybridization of N and O 2p levels with Zn and Ga 3d levels is studied by comparing our anion and cation X-ray spectra. The reduction in band gap is measured using a combination of XES and XAS for a wide range of Zn/O concentration (x = 0.06 → 0.42). We also use the above measurements to present a detailed description of the valence energy band composition in a binding energy picture.

In addition to X-ray spectroscopy, DFT calculations of previously proposed oxynitride superlattice structures[10,17] were performed using the WIEN2K code,[22] a full-potential linear augmented plane-wave plus local-orbital (LAPW+lo) code. The generalized gradient approximation (GGA) of Perdew−Burke−Ernzerhof[23] was used as the DFT functional, and an additional Hubbard potential U = 7.5 eV (GGA+U) was used to correct for the spin correlation of 3d orbitals in Ga and Zn. The U value used was in line with the U = 7 eV used by Huda et al.[21] but increased to better reproduce the measured energy gap between the valence band and lower energy sub-bands. Crystal structures from previous theoretical works were used as the basis of calculation: for $x \to 0$ a single O was introduced into a 108 atom GaN supercell, as performed by Yoshida et al.,[10] while for $x \approx 0.5$ the superlattice structure used by Jensen et al.[17] was used to give concentrations x = 0.5 and x = 0.43. All structures were optimized to minimize internal forces. The self-consistent calculations were then used to prepare simulated X-ray emission spectra for comparison with our experimental spectra using the XSPEC code included with WIEN2k.[24]

EXPERIMENT

The samples of $(Ga_{1-x}Zn_x)(N_{1-x}O_x)$ for x = 0.06−0.42 were prepared from a physical mixture of α-Ga_2O_3 (99.9%, High Purity Chemicals, Japan) and ZnO (99%, Kanto Chemicals, Japan; 97%, Wako Pure Chemicals, Japan). The initial mixture was heated to a specified temperature (1123−1223 K) at a rate of 10 K/min and then maintained at that temperature for 0.25−50 h under NH_3 flow (250 mL min^{-1}).[5] The initial molar ratio of zinc to gallium in each mixture was 1.0. After nitridation, the samples were cooled to room temperature under NH_3 flow. Preparation of each measured sample is summarized in Table 1. The resulting samples were characterized by SEM, TEM, XRD, and EDS and were shown to be well-crystallized submicrometer powders with a wurtzite crystal structure, as previously reported.[5]

Table 1. Preparation Conditions for $(Ga_{1-x}Zn_x)(N_{1-x}O_x)$ Samples

sample	initial Zn/Ga ratio	temperature (K)	time (h)	x
GAZN42	1.0	1223	0.5	0.42
GAZN18	1.0	1123	12.0	0.18
GAZN06	1.0	1123	50.0	0.06

Soft X-ray emission spectroscopy measurements were performed at Beamline 8.0.1 at the Advanced Light Source at the Lawrence Berkeley National Laboratory. Beamline 8.0.1 is equipped with a fluorescence endstation utilizing a Rowland-circle type spectrometer for resolving the energy of emitted X-rays as an synchrotron X-ray excited sample relaxes to the ground state.[25] Samples were oriented with a 30° angle between the incident radiation and the surface normal, and the emission spectrometer was fixed at 90° to the incident radiation. The spectrometer achieved a resolving power of 1000 ($E/\Delta E$). The spectrometer entrance slit and the monochromator exit slit were aligned in the vertical direction, while the exciting synchrotron radiation was horizontally polarized. XES measurements were collected using nonresonant excitation at X-ray beam energies above the associated absorption edge of the element in question (Zn: 1070 eV, O: 550 eV, N: 420 eV).

Soft X-ray absorption spectroscopy was performed at the Spherical Grating Monochromator (SGM) beamline at the Canadian Light Source at the University of Saskatchewan.[26] Absorption total fluorescence yield (TFY) was measured using a channel plate fluorescence detector at 38° to the surface normal. Absorption total electron yield (TEY) of ground electrons replenishing X-ray generated photoelectrons was measured using a picoammeter. Samples were oriented with incident radiation at 0° to the surface normal and grounded using carbon tape.

RESULTS AND DISCUSSION

To understand the band gap reduction in the GaN:ZnO system, we must use our spectroscopic results to build an understanding of its valence level. By comparing common spectral features across the Zn L_3, O $K\alpha$, and N $K\alpha$ X-ray emission and absorption spectra of GaN:ZnO, we can investigate the structural nature of the material as well as possible sources of its band gap reduction.

Nitrogen and oxygen $K\alpha$ XES and XAS probe the distribution of each element's 2p states in the valence and conduction band, respectively, governed by the dipole selection rules. Oxygen 2p states will hybridize with semicore d-bands in the post transition metal oxides (such as ZnO, CdO, and HgO); these d-symmetry states can therefore be probed by O $K\alpha$ XES, where they will appear as low-energy sub-bands, as we have previously demonstrated.[27] As shown in Figure 1, the O $K\alpha$ emission spectrum of Ga_2O_3 shows such a sub-band (magnified portion) even though the Ga 3d states are located at much lower energy (at least 9 eV) than Zn's 3d states. We also

dx.doi.org/10.1021/jp301231p | J. Phys. Chem. C 2012, 116, 7694−7700

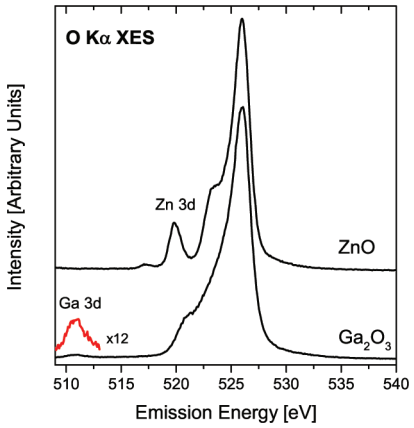

Figure 1. Oxygen $K\alpha$ XES of ZnO compared with Ga_2O_3. Hybridization with states of the associated metal center can be observed, providing an indication of the relative binding energy of these metal states. Ga 3d states are enlarged for clarity.

note that there is no feature at that energy in ZnO, making it clear that emission measured at this energy uniquely identifies O hybridization with Ga 3d states. We should therefore expect to find evidence of Ga states at this energy in the O $K\alpha$ spectra of GaN:ZnO if Ga−O hybridization is in fact occurring.

XPS measurements of the Zn 2p and O 1s binding energies are available for $(Ga_{1-x}Zn_x)(N_{1-x}O_x)$ at $x \leq 0.15$,[19] allowing us to align the Zn L_3 XES (a 3d4s → $2p_{3/2}$ transition) and O $K\alpha$ XES (a 2p → 1s transition) spectra of GAZN42 on a common energy axis, as shown in Figure 2. The XPS binding energy

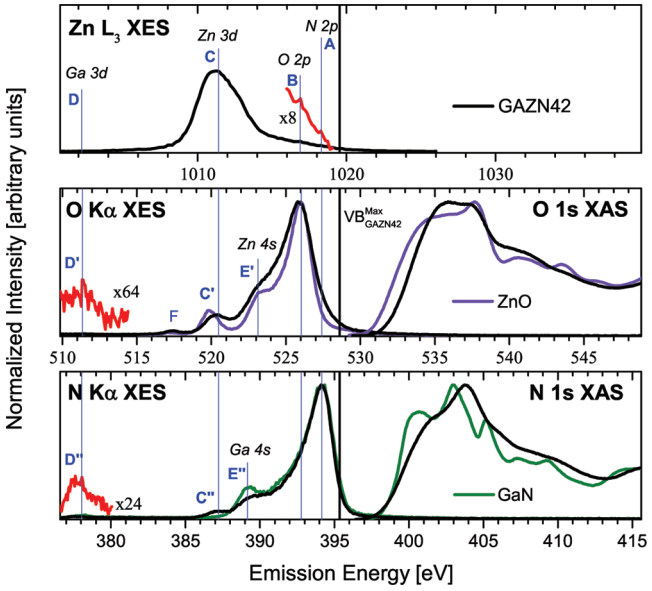

Figure 2. Comparison of Zn L_3, O $K\alpha$, and N $K\alpha$ XES of $(Ga_{1-x}Zn_x)(N_{1-x}O_x)$ at $x = 0.42$. The precursor materials, GaN and ZnO, are also plotted for comparison. The spectra have been aligned to demonstrate hybridization of Zn states (labeled C, C′, C″) and Ga states (D′ and D″) with the N and O 2p states. This allows us to consider the relative binding energy of all near-Fermi level states. Peak F is second order Zn L_2 emission and does not represent O DOS.

difference of the core levels in these two spectra is 490.9 eV, identically the difference in emission energy between the primary Zn L_3 emission peak at 1011.3 eV (labeled C) and a secondary O $K\alpha$ emission peak at 520.4 eV (C′). This secondary peak shows Zn 3d hybridization on the O $K\alpha$ measurement, and a small feature on the Zn L_3 spectrum at 1016.9 eV (magnified at B) is in close alignment with the primary O emission peak at 525.8 eV (a difference of 491.1 eV). This position is in alignment with ZnO's O emission peak at 526.0 eV, suggesting that the Zn in GAZN42 primarily sees O as a nearest neighbor in a ZnO phase. A low-intensity peak at an emission energy of 511.4 eV (labeled D′) is observed at the same energy as in Ga_2O_3, confirming Ga 3d−O hybridization is occurring. The separation of this Ga 3d peak and the Zn 3d peak (C′) is 9.0 eV.

The N $K\alpha$ spectrum of GAZN42 can be aligned to the common energy axis in Figure 2 through a band at emission energy 378.1 eV (labeled D″). This band occurs due to mixing of Ga 3d and N 2p states as first described in GaN.[28] This peak was not observed to shift in energy across the samples of GaN:ZnO studied from the position in GaN; this is not surprising as this band is sufficiently below the valence band to be composed of semicore states as well. This allows us to use Ga 3d as an anchor point in binding energy to align and compare the O $K\alpha$ and N $K\alpha$ XES in the absence of a definitive N 1s binding energy measurement of the GaN:ZnO system by aligning D″ with D′ (giving a binding energy difference between the N 1s and O 1s levels of 133.3 eV). The GAZN42 N $K\alpha$ spectra also exhibits a peak (labeled C″ at 387.0 eV) that is absent in pure GaN and can be attributed to N 2p−Zn 3d hybridization. This peak corresponds in binding energy to the main Zn L_3 peak (C at 1011.3 eV) using the alignment discussed above to an agreement of 0.1 eV, supporting the alignment scheme. The relative intensity of this peak increases with increasing Zn concentration as shown in Figure 3. This shows increased Zn−N bonding as the Zn concentration increases.

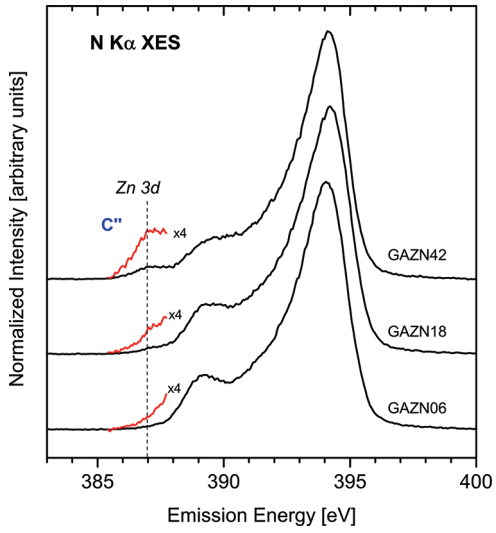

Figure 3. Comparison of N $K\alpha$ XES for $(Ga_{1-x}Zn_x)(N_{1-x}O_x)$ for $x = 0.06$−0.42. The intensity of the Zn 3d contribution (labeled C″) increases with increasing Zn concentration.

AN OXYNITRIDE SUPERLATTICE OR A SOLID SOLUTION?

While the valence band description we have built in Figure 2 displays evidence of both the Ga and Zn sites in the system bonding with both the O and N present, it is possible to rule out the possibility of an oxynitride superlattice structure by careful consideration of the valence band features. As both the

dx.doi.org/10.1021/jp301231p | J. Phys. Chem. C 2012, 116, 7694−7700

O 2p and N 2p peaks have similar symmetry and occur close together in energy at the top of the valence band, it is expected that these states would hybridize if they were part of a homogeneous oxynitride structure. Despite O and N not being nearest neighbors, the periodic nature of a superlattice would allow these states to delocalize throughout the crystal structure and interact where they are coincident in energy. This expected interaction can be observed in our calculated X-ray spectra, as displayed in Figure 4, in two ways: the N peak should be

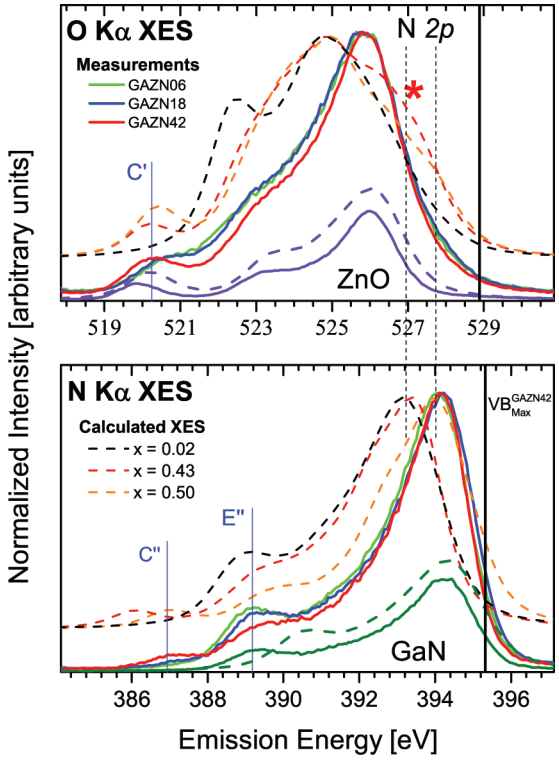

Figure 4. Calculated X-ray emission spectra (dashed lines) versus experimental measurements (solid lines). The calculated spectra predict a shoulder (marked with an asterisk) on the high-energy side of the O *Kα* peak from hybridization with N 2p states, as well as increased repulsion of the N *Kα* peak to higher energy with increasing O composition. Neither effect is observed in the experimental measurements; instead the primary peak of the GaN:ZnO XES measurements most closely resembles pure GaN and ZnO, confirming GaN:ZnO behaves as a heterojunction solid solution of GaN and ZnO (shown beneath for comparison).

repelled to higher orbital energy as more O is introduced into the system, and the O peak should have a shoulder on the high-energy side corresponding to the N peak and that decreases in spectral weight as the ratio of O versus N increases; neither effect is observed in the experimental spectra. Indeed, there are no significant changes in the primary O and N peaks, which instead agree well with the measurements of powdered ZnO and GaN, but broader and shifted in energy. As Zn/O concentration increases, the Zn peak C′ in the O spectra shifts down in energy, separating from the valence band (as in ZnO), while the Ga 4s peak E″ in the N spectra decreases in intensity as the Zn 3d peak C″ increases, due to Zn displacing Ga as a nearest neighbor. This experimental evidence contradicts key features of the superlattice DFT calculations, strongly suggesting that the GaN:ZnO bulk crystal structure is not a homogeneous oxynitride superlattice.

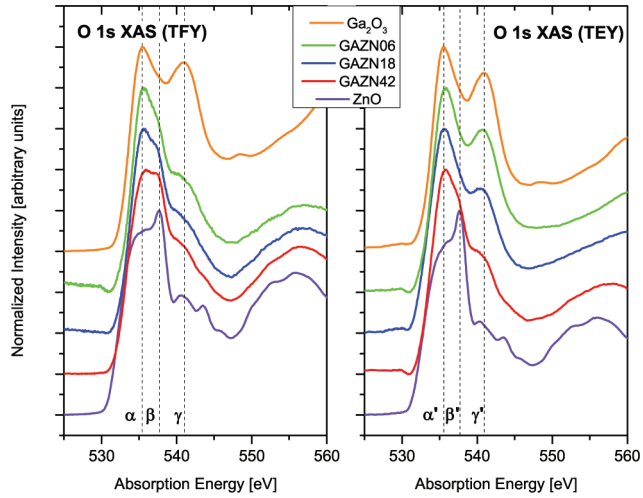

Figure 5. O 1s XAS total fluorescence yield (TFY) peak *β* indicates the contribution of ZnO-like O conduction band states within the sample at $x = 0.42$. This contribution is reduced with decreasing x. This is in contrast to the O 1s XAS total electron yield peak *γ′*, which indicates the dominance of Ga−O bonding on the surface of the GaN:ZnO samples.

Discounting the superlattice structure, how should the GaN:ZnO structure be considered? Figure 5 shows the TFY (bulk sensitive) and TEY (surface sensitive) O 1s XAS measurements, which show the progression from ZnO to Ga_2O_3 from bottom to top. As the material undergoes nitridation, excess ZnO is eliminated, causing feature *β* to be extinguished while feature *α* grows. Ga_2O_3 takes over as the primary oxygen species at low Zn content, but for samples GAZN42 and GAZN18 there remains a sizable fraction of ZnO in the bulk. However, on the surface, *β′* is largely extinguished even in GAZN42, while feature *γ′* is pronounced, indicating the surface oxide layer is primarily Ga_2O_3. This reveals that the GaN:ZnO system across this concentration range is a solid solution of ZnO phases contained within a GaN host. The Zn−N and Ga−O bonding observed in the XES measurements is explained by interactions at the phase boundary indicative of a heterojunction, which will also explain the band gap reduction.

■ ORIGIN OF BAND GAP REDUCTION

The near-valence electronic structure details derived from Figure 2 can be used to investigate the origin of the observed band gap reduction within the GaN:ZnO system. The figure shows that the upper-energy edge of the O and N *Kα* emission curves overlap in energy, which is not surprising considering both correspond to the top of a common, delocalized valence band in the phase-boundary region of the material. However, the dominant feature of the N *Kα* XES (peak A in Figure 2) is located at higher energy than that of the O *K* XES (peak B), indicating that nitrogen 2p states dominate the highest-energy states of the valence band. In our XES measurements, we do not observe an energy shift with concentration changes in either the O or N valence band edge as would be expected if N 2p−Zn 3d or O 2p−Ga 3d repulsion was a dominant effect, ruling this out as a factor in band gap reduction as Zn/O concentrations change.

In Figure 6, we show the Zn $L_{2,3}$ XES measurements for GAZN42 and GAZN06, the extremes of Zn composition in our study. The intensity ratio of the L_2 peak to the L_3 peak can be

dx.doi.org/10.1021/jp301231p | J. Phys. Chem. C 2012, 116, 7694−7700

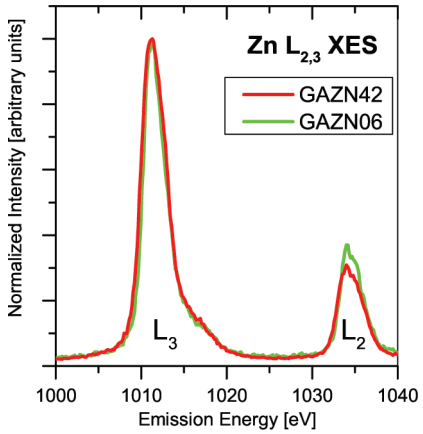

Figure 6. Zn $L_{2,3}$ XES of $(Ga_{1-x}Zn_x)(N_{1-x}O_x)$ for x = 0.06 and 0.42. While there is a small change in relative peak intensity, no features appear that would suggest the creation of new Zn defect states at higher concentration.

seen to decrease slightly with increased Zn. By integrating under each peak, an intensity ratio $I(L_2)/I(L_3)$ can be found, which decreases with increased Zn content, from 0.3111 in GAZN06 to 0.2675 in GAZN42. L_2 and L_3 X-ray emission spectra from 3d elements correspond to X-ray transitions from occupied 3d4s valence states to $2p_{1/2}$ and $2p_{3/2}$ core vacancies, respectively. The reduction of the L_2 to L_3 intensity ratio with increased Zn can be linked to an increased number of charge carriers with ZnO substitution.[29] The number of free charge carriers in a semiconductor is expected to increase as its band gap decreases (given constant temperature), suggesting the L_2 to L_3 intensity ratio can be used as an additional spectroscopic test to indicate band gap reduction in the GaN:ZnO system. Apart from this change in intensity ratio, no new structure emerged in the Zn $L_{2,3}$ XES at increased Zn composition that would suggest the emergence of a Zn acceptor or defect levels that could affect the optical band gap.

Figure 7 shows the N and O emission and absorption spectra in the vicinity of the band gap. As the Zn/O concentration increases, both the N and O conduction band (CB) edges are repelled to lower energy, with the N CB states offset below the O CB states by 0.2 eV. The CB minima are both shifted from the isolated precursor materials and would connect on the phase boundary, as depicted in Figure 8 for sample GAZN42 and its GaN and ZnO phases. As shown in Figure 2, the isolated ZnO XAS onset occurs at lower orbital energy than that of isolated GaN, but the GaN onset is sharper, with more spectral weight at lower energy (and hence a greater density of states). In the vicinity of the ZnO/GaN phase boundary the overlap of these bands in energy will lead to state repulsion. As GaN exists at higher concentration in all samples tested, and has a greater spectral weight at lower orbital energy, its states dominate and repel the ZnO CB states to higher orbital energy. However, as ZnO concentration increases, the N CB onset is itself repelled to lower orbital energy, always staying below the O CB onset. The overall effect is a 0.4 eV shift downward in CB onset energy from low to high Zn concentration (x = 0.06 → 0.42) in the solid solution. On the other hand, the VB maximum does not undergo such a shift as concentration changes, owing to the greater energy separation of the occupied N and O 2p bands. The VB maximum of the solid solution is composed primarily of N 2p states in the GaN phase, but there are still contributions from O 2p as well as a small amount of

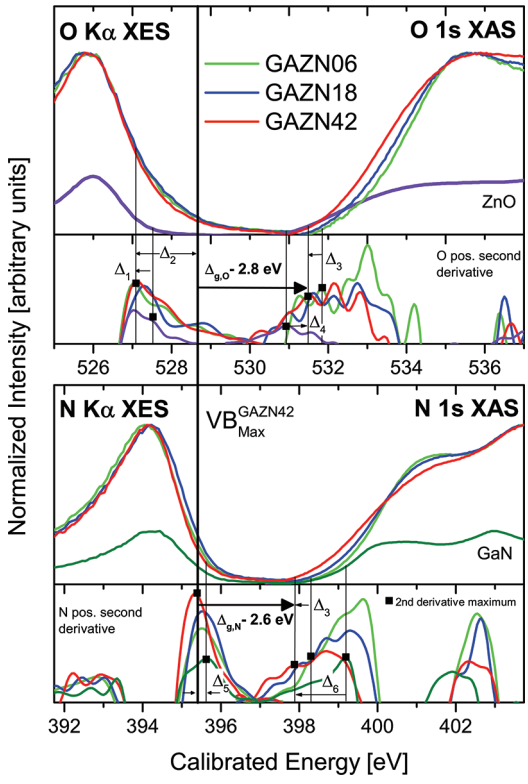

Figure 7. Band gap region of nitrogen and oxygen $K\alpha$ emission and absorption spectra of $(Ga_{1-x}Zn_x)(N_{1-x}O_x)$ for all samples, with a positive second derivative of each spectrum plotted beneath. There is no significant shift in valence band onset between x = 0.06 and 0.42, but using the second derivative of N 1s XAS we measure a 0.4 eV reduction in band gap of GAZN42 (relative to GAZN06) in the conduction band onset energy. Energy offsets are summarized in Table 2.

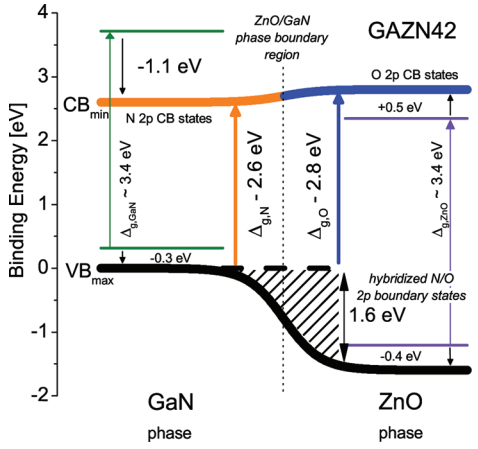

Figure 8. Proposed band transition scheme for $(Ga_{1-x}Zn_x)(N_{1-x}O_x)$ at x = 0.42, showing two transitions in GaN and ZnO components of the solid solution (2.6 and 2.8 eV, in agreement with UV−vis measurements). Valence and conduction band energy shifts from the precursor isolated GaN and ZnO to the solid solution phases are shown. The band edges of GaN are forced to lower energy within an expanded ZnO gap by state repulsion.

Zn 3d. While the main O 2p peak occurs at slightly lower orbital energy than isolated ZnO, hybridization at the phase interface broadens this O band sufficiently that transitions to the ZnO phase CB are possible, allowing the higher-energy transition observed in PL measurements of the system.[10] At the phase boundary the system acts as if the GaN band edges are

dx.doi.org/10.1021/jp301231p | J. Phys. Chem. C 2012, 116, 7694−7700

"wedged" between the ZnO band edges, with repulsive forces lowering the overall energy gap of the GaN. Rigid band behavior causes these phase boundary interactions to be transmitted into the interior of these phases, resulting in the overall shift of the majority of states that would occur in the "interior" of GaN and ZnO phases (although unknown size effects would play a significant role in determining the electronic structure within each phase).

Using the second derivatives of the X-ray spectra we can choose comparable CB and VB onset points from the various spectra that correspond to a significant onset of states at that energy. The highest-/lowest-energy local maximum in the second derivative of an XES/XAS spectrum has been shown to be a useful estimate of energy band onset in post-transition-metal oxides[27] and is used to combat experimental broadening factors inherent to monochromators and spectrometers, as well as the energy uncertainty related to the short lifetime of the excited core state. Similar second derivative features are also used to estimate the energy of onset features across multiple samples. Energy band offsets of note are summarized in Table 2 and depicted in Figure 8.

Table 2. Energy Band Offsets As Measured by the Second Derivative

offset	energy offset (±0.1 eV)	description
Δ_1	−0.4	main O 2p peak from ZnO to GAZN42
Δ_2	1.6	N 2p−O 2p onset difference for GAZN42
Δ_3	0.4	band gap shift with concentration (x = 0.06 → 0.42)
Δ_4	0.5	O CB edge shift from ZnO to GAZN42
Δ_5	−0.3	N VB edge shift from GaN to GAZN42
Δ_6	−1.1	N CB edge shift from GaN to GAZN42
$\Delta_{g,GaN}$	≈3.4	GaN energy gap
$\Delta_{g,ZnO}$	≈3.4	ZnO energy gap
$\Delta_{g,O}$	2.8	ZnO phase energy gap
$\Delta_{g,N}$	2.6	GaN phase energy gap

The overall result of the above is an energy gap of 2.6 eV associated with the GaN phase and 2.8 eV with the ZnO phase. While the XAS spectra measure the CB states as perturbed by an X-ray induced core hole, the N XAS onset consists of states from the GaN phase of the material, which has a CB onset that does not undergo an energy shift in the presence of a core hole (as confirmed by our DFT calculations of a 2 × 2 × 2 supercell of GaN with one core electron removed from a N site). These band gap results are in good agreement with the UV−vis diffuse reflectance measurements[2] and qualitatively agree with the two photoluminescent peaks described by Yoshida et al.[10] Our results are also in agreement with previous theoretical studies on the band gap reduction in the GaN:ZnO system[20,21] which found the band gap reduction within the GaN:ZnO system to arise from a decrease in CB onset energy (as opposed to an increased VB maximum energy) in a solid solution structure.

A DUAL BAND GAP HETEROSTRUCTURE

Considering the GaN:ZnO solid solution as a heterostructure allows it to be compared to explicitly manufactured GaN:ZnO layered structures that have attracted interest as possible blue/UV emitting optoelectronic devices.[30−32] An X-ray and ultraviolet photoelectron spectroscopy (XPS/UPS) study of heterostructures produced by molecular beam epitaxy (MBE)[30] has demonstrated occupied band offsets comparable to the current study, most specifically a binding energy difference between the Ga 3d−Zn 3d peaks of 9.4 eV (compared to 9.0 eV in the present study). LEDs produced from GaN/ZnO heterostructures show 550−600 nm (2.25−2.07 eV) emission which is attributed to defects,[32] suggesting that size and interface effects may be important to our proposed mechanism for GaN:ZnO band gap reduction. Further study is warranted, especially in characterizing the length scale of the GaN:ZnO heterojunction that prevents re-establishment of the bulk GaN/ZnO band gaps. The comparison of this length scale to other relevant length scales (i.e., exciton diffusion length) may offer the opportunity to tune the material for photocatalytic and other applications.

The dual band gap nature of GaN:ZnO also presents opportunities to further optimize its quantum efficiency as a photocatalyst. In general, multiple band gap solar cells are better able to absorb and retain the energy of photons with higher wavelengths, leading to fewer thermodynamic losses.[33] Additionally, the inverted nature of this heterojunction as shown in Figure 8, where a smaller energy gap is contained within a larger one, has been shown to increase the available photocurrent within a semiconductor/electrolyte cell.[34] As we are interested in driving redox reactions with fixed chemical potentials, additional photocurrent is preferred over unnecessary photovoltage that will be lost to thermal processes. Indeed, a material system with two independently tunable band gaps could theoretically provide valence and conduction band edges optimized for a variety of redox reactions while simultaneously providing a desired band gap. Investigation of methods to better control the electronic structure of GaN:ZnO, particularly the composition of the valence band maximum, could prove very useful in producing a better photocatalyst.

CONCLUSIONS

We have presented a binding energy picture showing the near Fermi level electronic structure of GaN:ZnO by means of soft X-ray emission and absorption spectroscopy. Our analysis of this structure allows us to conclude that:

1. The GaN:ZnO samples measured are best described as a solid solution heterostructure of GaN and ZnO phases, as O−N hybridization predicted by DFT models is not observed near the Fermi level.
2. The valence band consists of, from highest to lowest energy, N 2p, O 2p, Zn 3d, and Ga 3d states in accordance with previous band structure calculations for this system.[10,17]
3. N 2p−Zn 3d and O 2p−Ga 3d hybridization occurs in the compound and can be observed by the presence of low-energy peaks in the N and O $K\alpha$ XES that are not present in GaN and ZnO. This hybridization would occur along phase boundaries as described by Huda et al.[21]
4. The repulsion of O/N 2p and Ga/Zn 3d states on the phase boundaries does not lead to an increase in the energy of the valence band edge across the sample compositions studied, and no changes were observed in the Zn $L_{2,3}$ emission spectra that could be attributed to the formation of a Zn acceptor or defect level.
5. Instead, the mechanism of band gap reduction is repulsion between empty conduction band states associated with the distinct phases of the material, forcing empty

dx.doi.org/10.1021/jp301231p | J. Phys. Chem. C 2012, 116, 7694−7700

N 2p states to lower orbital energy. This causes the GaN:ZnO boundary region to behave as an inverted heterojunction as shown in Figure 8.

6. We have estimated two optical band gaps of 2.6 and 2.8 eV for the $(Ga_{1-x}Zn_x)(N_{1-x}O_x)$ (x = 0.42) solid solution using the second derivatives of X-ray emission and absorption spectra. The CB of each phase in the material would connect at the phase boundary, leading to the two possible band transitions in the phase boundary region. This result is in agreement with previous optical measurements of both the band gap[2] and multiple luminescent transitions[5] as well as theoretical calculations showing CB energy shifting to be the critical factor in overal band gap reduction of the system.[20,21]

AUTHOR INFORMATION

Corresponding Author

*E-mail: eamon.mcdermott@usask.ca.

Notes

The authors declare no competing financial interest.

ACKNOWLEDGMENTS

We gratefully acknowledge support from the Natural Sciences and Engineering Research Council of Canada (NSERC), the Canada Research Chair program, the Russian Science Foundation for Basic Research (Project 11-02-00022), and the Core Research for Evolutional Science and Technology (CREST) and Solution Oriented Research for Science and Technology (SORST) programs of the Japan Science and Technology Corporation (JST). Measurements described in this work were performed at the Canadian Light Source, which is supported by NSERC, the National Research Council Canada, the Canadian Institutes of Health Research, the Province of Saskatchewan, Western Economic Diversification Canada, and the University of Saskatchewan. The Advanced Light Source is supported by the Director, Office of Science, Office of Basic Energy Sciences of the US Department of Energy under Contract No. DE-AC02-05CH11231. Computing resources were provided by WestGrid and Compute/Calcul Canada.

REFERENCES

(1) Maeda, K.; Teramura, K.; Lu, D.; Takata, T.; Saito, N.; Inoue, Y.; Domen, K. *Nature* **2006**, *440*, 295.

(2) Maeda, K.; Teramura, K.; Takata, T.; Hara, M.; Saito, N.; Toda, K.; Inoue, Y.; Kobayashi, H.; Domen, K. *J. Phys. Chem. B* **2005**, *109*, 20504−20510.

(3) Bard, A. J.; Fox, M. A. *Acc. Chem. Res.* **1995**, *28*, 141−145.

(4) Maeda, K.; Domen, K. *J. Phys. Chem. C* **2007**, *111*, 7851−7861.

(5) Maeda, K.; Domen, K. *Chem. Mater.* **2010**, *22*, 612−623.

(6) Srikant, V.; Clarke, D. R. *J. Appl. Phys.* **1998**, *83*, 5447−5451.

(7) Ejder, E. *Phys. Status Solidi A* **1971**, *6*, 445−448.

(8) Maeda, K.; Takata, T.; Hara, M.; Saito, N.; Inoue, Y.; Kobayashi, H.; Domen, K. *J. Am. Chem. Soc.* **2005**, *127*, 8286−8287.

(9) Wang, J.; Huang, B.; Wang, Z.; Wang, P.; Cheng, H.; Zheng, Z.; Qin, X.; Zhang, X.; Dai, Y.; Whangbo, M.-H. *J. Mater. Chem.* **2011**, *21*, 4562−4567.

(10) Yoshida, M.; Hirai, T.; Maeda, K.; Saito, N.; Kubota, J.; Kobayashi, H.; Inoue, Y.; Domen, K. *J. Phys. Chem. C* **2010**, *114*, 15510−15515.

(11) Han, W.-q.; Ward, M. J.; Sham, T. *J. Phys. Chem. C* **2011**, *115*, 3962−3967.

(12) Maeda, K.; Hashiguchi, H.; Masuda, H.; Abe, R.; Domen, K. *J. Phys. Chem. C* **2008**, *112*, 3447−3452.

(13) Tran, F.; Blaha, P. *Phys. Rev. Lett.* **2009**, *102*, 226401.

(14) Wei, S.-H.; Zunger, A. *Phys. Rev. B* **1988**, *37*, 8958−8981.

(15) Schröer, P.; Krüger, P.; Pollmann, J. *Phys. Rev. B* **1993**, *47*, 6971−6980.

(16) Van de Walle, C. G.; Neugebauer, J. *Appl. Phys. Lett.* **1997**, *70*, 2577−2579.

(17) Jensen, L.; Muckerman, J.; Newton, M. *J. Phys. Chem. C* **2008**, *112*, 3439−3446.

(18) Hirai, T.; Maeda, K.; Yoshida, M.; Kubota, J.; Ikeda, S.; Matsumura, M.; Domen, K. *J. Phys. Chem. C* **2007**, *111*, 18853−18855.

(19) Mapa, M.; Thushara, K. S.; Saha, B.; Chakraborty, P.; Janet, C. M.; Viswanath, R. P.; Madhavan Nair, C.; Murty, K. V. G. K.; Gopinath, C. S. *Chem. Mater.* **2009**, *21*, 2973−2979.

(20) Li, L.; Muckerman, J.; Hybertsen, M.; Allen, P. *Phys. Rev. B* **2011**, *83*, 134202.

(21) Huda, M.; Yan, Y.; Wei, S.-H.; Al-Jassim, M. *Phys. Rev. B* **2008**, *78*, 195204.

(22) Blaha, P.; Schwarz, K.; Madsen, G.; Kvasnicka, D.; Luitz, J. *WIEN2k, an augmented plane wave + local orbitals program for calculating crystal properties*; Karlheinz Schwarz, Techn. Universitat Wien: Austria, ISBN: 3-9501031-1-2, 2001.

(23) Perdew, J. P.; Burke, K.; Ernzerhof, M. *Phys. Rev. Lett.* **1996**, *77*, 3865−3868.

(24) Schwarz, K.; Neckel, A.; Nordgren, J. *J. Phys. F: Met. Phys.* **1979**, *9*, 2509−2521.

(25) Jia, J. J.; Callcott, T. A.; Yurkas, J.; Ellis, A. W.; Himpsel, F. J.; Samant, M. G.; Stöhr, J.; Ederer, D. L.; Carlisle, J. A.; Hudson, E. A.; Terminello, L. J.; Shuh, D. K.; Perera, R. C. C. *Rev. Sci. Instrum.* **1995**, *66*, 1394−1397.

(26) Regier, T.; Krochak, J.; Sham, T. K.; Hu, Y.; Thompson, J.; Blyth, R. *Nucl. Instrum. Methods Phys. Res., Sect. A* **2007**, *582*, 93−95.

(27) McLeod, J. A.; Wilks, R. G.; Skorikov, N. A.; Finkelstein, L. D.; Abu-Samak, M.; Kurmaev, E. Z.; Moewes, A. *Phys. Rev. B* **2010**, *81*, 245123.

(28) Stagarescu, C.; Duda, L.; Smith, K.; Guo, J.; Nordgren, J.; Singh, R.; Moustakas, T. *Phys. Rev. B* **1996**, *54*, R17335−R17338.

(29) Chang, G. S.; Kurmaev, E. Z.; Boukhvalov, D. W.; Finkelstein, L. D.; Kim, D. H.; Noh, T.-W.; Moewes, A.; Callcott, T. A. *J. Phys.: Condens. Matter* **2006**, *18*, 4243−4251.

(30) Hong, S.-K.; Hanada, T.; Makino, H.; Chen, Y.; Ko, H.-J.; Yao, T.; Tanaka, A.; Sasaki, H.; Sato, S. *Appl. Phys. Lett.* **2001**, *78*, 3349−3351.

(31) Hwang, D.-K.; Kang, S.-H.; Lim, J.-H.; Yang, E.-J.; Oh, J.-Y.; Yang, J.-H.; Park, S.-J. *Appl. Phys. Lett.* **2005**, *86*, 222101.

(32) Ju-Young, L.; Jong Hoon, L.; Hong Seung, K.; Won Suk, H.; Hyung Koun, C.; Jin Young, M.; Ho Seong, L. *J. Korean Phys. Soc.* **2009**, *55*, 1568.

(33) Henry, C. H. *J. Appl. Phys.* **1980**, *51*, 4494−4500.

(34) Licht, S.; Khaselev, O.; Ramakrishnan, P. A.; Soga, T.; Umeno, M. *J. Phys. Chem. B* **1998**, *102*, 2546−2554.